[Frontiers in Bioscience 7, a60-71, April 1, 2002]

PRION PEPTIDE 106-126 AS A MODEL FOR PRION REPLICATION AND NEUROTOXICITY

Neena Singh, Yaping Gu, Sharmila Bose, Sudheera Kalepu, Ravi Shankar Mishra, and Susamma Verghese

The Institute of Pathology, Case Western Reserve University, 2085, Adelbert Road, Cleveland, Ohio

TABLE OF CONENTS

1. ABSTRACT

Prion diseases or transmissible spongiform encephalopathies are neurodegenerative disorders that are genetic, sporadic, or infectious. The pathogenetic event common to all prion disorders is a change in conformation of the cellular prion protein (PrP^{C}) to the scrapie isoform (PrP^{Sc}), which, unlike PrP^{C}, aggregates easily and is partially resistant to protease digestion. Although PrP^{Sc} is believed to be essential for the pathogenesis and transmission of prion disorders, the mechanism by which PrP^{Sc} deposits cause neurodegeneration is unclear. It has been proposed that in some cases of prion disorders, a transmembrane form of PrP, termed ^{Ctm}PrP may be the mediator of neurodegenerative changes rather than PrP^{Sc} *per se*. In order to understand the underlying cellular processes by which PrP^{Sc} mediates neurodegeneration, we have investigated the mechanism of neurotoxicity by a β-sheet rich peptide of PrP in a cell model. We show that exposure of human neuronal cell lines NT-2 and M17 to the prion peptide 106-126 ($PrP^{106-126}$) catalyzes the aggregation of endogenous cellular prion protein (PrP^{C}) to an amyloidogenic form that shares several characteristics with PrP^{Sc}. Intracellular accumulation of these PrP^{Sc}-like forms upregulates the synthesis of ^{Ctm}PrP, which is proteolytically cleaved in the endoplasmic reticulum and the truncated C-terminal fragment is transported to the cell surface. In addition, we have isolated mutant NT-2 and neuroblastoma cells that are resistant to toxicity by $PrP^{106-126}$ to facilitate further characterization of the biochemical pathways of $PrP^{106-126}$ neurotoxicity. The $PrP^{106-126}$-resistant phenotype of these cells could result from aberrant binding or internalization of the peptide, or due to an abnormality in the downstream pathway(s) of neuronal toxicity. Thus, our data suggest that PrP^{Sc} aggregation occurs by a process of 'nucleation' on a pre-existing 'seed' of PrP. Furthermore, the $PrP^{106-126}$-resistant cells reported here will provide a unique opportunity for identifying the cellular and biochemical pathways that mediate neurotoxicity by PrP^{Sc}.

2. INTRODUCTION

Prion disorders occur when a normally expressed surface glycoprotein, the prion protein (PrP^{C}), changes its

conformation from a predominantly α-helical to a β-sheet rich form that is pathogenic (PrP^{Sc}). This transformation is caused by an exogenous source of PrP^{Sc} in infectious disorders, is triggered by prion protein gene mutations in the inherited forms, and is believed to be a random, spontaneous event the case of sporadic disorders. After the initial conversion, subsequent conversion of additional PrPC molecules occurs spontaneously, resulting in PrPSc deposits in the brain parenchyma. PrP^{Sc} differs from PrP^{C} in several biophysical characteristics, such as increased aggregability and resistance to protease digestion. Amyloid deposits comprised of PrP^{Sc} are one of the principal causes of neuronal toxicity in prion disorders (1-4).

Neurodegenerative changes typical of prion diseases are also seen without detectable PrP^{Sc}, suggesting the presence of alternative mechanisms of neuronal death in prion disorders in addition to PrP^{Sc} (5-7). One of these mechanisms is through ^{Ctm}PrP, a transmembrane form of PrP that spans the endoplasmic reticulum (ER) membrane at residues 113-135 with its N-terminus in the cytosol, instead of the normal glycolipid (GPI)-linked PrP^{C} that is translocated co-translationally into the ER lumen. Mice carrying the mutant PrP transgene A117V that leads to increased synthesis of ^{Ctm}PrP rather than GPI-linked PrP^{C} show spontaneous neurodegeneration without detectable PrP^{Sc}, and show neurodegeneration earlier and with smaller amounts of accumulated PrP^{Sc} than the corresponding animals with a deleted transmembrane domain when challenged with infectious prions. In these cases the extent of neurodegeneration co-relates directly with the amount of ^{Ctm}PrP, not the PrP^{Sc} load, indicating that ^{Ctm}PrP, and not the accumulated PrP^{Sc} mediates neurodegeneration in these cases (8, 9).

In this report, we describe one of the possible mechanisms of PrP^{C} to PrP^{Sc} conversion, and the co-relation between PrP^{Sc} accumulation and ^{Ctm}PrP generation. For causing the aggregation of PrP^{C}, an internal peptide of PrP including residues 106-126 ($PrP^{106-126}$) was used to replace the proteinase K (PK)-resistant fragment of PrP^{Sc} that is the principal constituent of the infectious prion particle. $PrP^{106-126}$ offers several advantages over PrP^{Sc}. It is similar to PrP^{Sc} in several ways, and at the same time is more soluble and easy to manipulate for cell culture studies. For example, like PrP^{Sc}, $PrP^{106-126}$ is rich in β-sheet structure, forms aggregates that are detergent insoluble and PK-resistant, and is toxic to primary cultures of neurons (10-12). Furthermore, residues 90-141 of PrP are sufficient for initiating or blocking the transformation of PrP^{C}, probably because this is the principal site of PrP^{Sc} and PrP^{C} binding during the conversion process (13-16). This region can be further narrowed down to residues 112-120, which are considered particularly important for the binding and inhibitory effect (12, 15). Using this peptide, several PrP binding proteins have been identified on neuronal cells, including glial fibrillary acidic protein (GFAP), Bcl-2, a 66kDa membrane protein, and the 37kDa laminin receptor precursor protein (17, 18). Recently, $PrP^{106-126}$ has been shown to interact with α- and β-tubulin, with the suggestion that the toxic effects of this fragment are mediated by altering intracellular calcium homeostasis (44).

We show that exposure of PrP^{C}-expressing NT-2 and neuroblastoma cells to non-toxic concentrations of $PrP^{106-126}$ for prolonged periods of time initiates the co-aggregation of PrP^{C} into amyloidogenic PrP^{Sc}-like forms that accumulate in lysosomes. Consequently, there is increased synthesis of the potentially neurotoxic transmembrane form of PrP (^{Ctm}PrP) in these cells. In a separate set of experiments, we exposed chemically mutagenized neuroblastoma and NT-2 cells to toxic doses of $PrP^{106-126}$, and isolated mutants that are resistant to toxicity by this peptide. Since the PrP residues 106-126 play an important role in the interaction of PrP^{Sc} with PrP^{C}, the mutant cell clones probably represent a disruption in the binding, or a downstream pathway of cellular toxicity by $PrP^{106-126}$. An analysis of these mutants will help in identifying PrP-binding receptor(s) and the biochemical pathways of neurotoxicity by $PrP^{106-126}$, information that is critical for the development of inhibitors of PrP^{Sc}-mediated neuronal death. Thus, this study provides the first direct evidence for nucleation-dependent transformation of PrP^{C} to a PrP^{Sc}-like form in a cell model, and shows a direct correlation between intracellular PrP^{Sc} accumulation and ^{Ctm}PrP upregulation, confirming the role of ^{Ctm}PrP as an important mediator of prion-related neuropathology. In addition, the $PrP^{106-126}$-resistant neuronal cells described in this report will provide an important experimental tool for identifying the specific biochemical pathways that mediate toxicity by $PrP^{106-126}$, and by extrapolation, PrP^{Sc}.

3. MATERIALS AND METHODS

3.1. Materials and cell culture conditions

All cell culture supplies were obtained from Invitrogen. Hygromycin B was from Calbiochem; Hoechst and lysotracker dye were from Molecular Probes (Eugene, Oregon). Biotinylated $PrP^{106-126}$ and scrambled $PrP^{106-126}$ were custom-synthesized (Genemed Corp., San Francisco, CA). Glutaraldehyde, osmium tetroxide, uranyl acetate, lead citrate, and Epoxy resin were from Polysciences Inc. (Warrington, PA). Anti-PrP monoclonal antibody 3F4 (specific to PrP residues 109-112) was from Richard Kascsak (New York State Institute for Basic Research in Developmental Disabilities). Anti-PrP monoclonal antibody 8H4 that binds to a site between residues 145-180 of PrP was raised in our facility (19). All other chemicals were purchased from Sigma. PrP^{C}-expressing human neuroblastoma cells were generated as described previously (20), and cultured in the presence of 500μg/ml of hygromycin B. NT-2 cells expressing high levels of PrP were isolated by repeated sub-cloning of cells obtained from ATCC.

3.2. Mutagenesis and selection of PrP106-126 resistant cells

The following peptides were custom-synthesized for the selection of $PrP^{106-126}$-resistant cells (Genemed Corp., San Francisco, CA): [1.] $PrP^{106-126}$: KTNMKHMAGAAAAGAVVGGLG ($PrP^{106-126}$), [2.] Scrambled $PrP^{106-126}$: NGAMALMGGHGATKVKVGAAA ($PrP^{Scr106-126}$), [3.] $PrP^{106-126}$ with a biotin tag at the N-terminus: Biotin—$PrP^{106-126}$, [4.] Scrambled $PrP^{106-126}$ with a biotin tag at the N-terminus: Biotin--$PrP^{Scm106-126}$.Biotinylated $PrP^{106-126}$ has been used for *in vitro* studies in neurons, and has been shown to retain the biochemical properties of the peptide (21). Peptide stocks were dissolved in DMSO, and kept frozen until use.

For prolonged culture in the presence of peptide, 5μM $PrP^{106-126}$ was used, as opposed to 80μM for selecting $PrP^{106-126}$-resistant cells.

First, PrP^{C}-expressing neuroblastoma (M17) and NT-2 cells were immunostained with anti-PrP antibody 3F4 and sorted by FACS analysis to select cells expressing high levels of PrP. These cells were expanded in culture and mutagenized by either ethyl-methyl-sulfonate (EMS, 150μg/ml) or N-methyl-N'-nitro-N-nitrosoguanidine (MNNG, 10 μg/ml). After culturing for 24 hours in the presence of these mutagens, the cells were washed and cultured in regular medium for 1 week. Cultures showing ~50% cell death after exposure to mutagens were grown in culture for one week to allow recovery from mutagen-induced toxicity, and exposed to $PrP^{106-126}$, $PrP^{Scm106-126}$ (80μM), or only solvent. The peptide-containing medium was changed every third day. Cell death was monitored by lactate dehydrogenase (LDH) assay of the culture medium every 24 hours. The cytotoxicity assay kit CytoTox96 was used for measuring LDH activity according to the manufacturer's instructions. Every week, the cells were trypsinized, re-plated, and supplemented with the peptides. Non-mutagenized M17 and NT-2 cells received a similar treatment, and were used as controls. Parallel cultures were exposed to biotin-$PrP^{106-126}$ and biotin-$PrP^{Scm106-126}$, and the cells were stained with Texas-red conjugated Streptavidin at different time points till the control, non-mutagenized cells finally died at ~6 weeks. In the initial two weeks of treatment, the cells treated with $PrP^{106-126}$ in fact proliferated. With continued treatment, the intracellular deposits of $PrP^{106-126}$ became larger, and the LDH activity released in the medium continued to increase. The number of apoptotic cells in the culture were determined by Hoechst staining (1 μg/ml dye; Molecular probes) and Tunnel assay (Oncor, Gaithersburg, MD) performed on a small aliquot of cells cultured separately on coverslips, according to the manufacturer's instructions. In short, MTT was added to the wells to a final concentration of 1 mg/ml, and incubated at 37°C for 3 hours. Cells were lysed with 20% SDS solution of 50% dimethylformamide, pH 4.7, incubated overnight at 37°C, and MTT reduction was determined colorimetrically at an OD of 550 nm. After six weeks of treatment with $PrP^{106-126}$, almost all of the non-mutagenized cells treated with $PrP^{106-126}$ died. Among the mutagenized cells, ~2% of the cells treated with $PrP^{106-126}$ survived, which started forming colonies. There was no effect on control or mutagenized cells treated with $PrP^{Scm106-126}$, or the solvent alone. In fact $PrP^{Scm106-126}$ could not be detected on the cell surface or in any intracellular compartment throughout the six weeks of treatment.

In a parallel set of dishes, non-mutagenized, NT-2 cells expressing high amounts of PrP^{C} or PrP^{C}-transfected neuroblastoma cells were cultured in the presence of non-toxic concentrations of $PrP^{106-126}$ (5μM), or the scrambled peptide for 1-12 months. At the time of sub-culture, biotin-tagged $PrP^{106-126}$ or biotin-tagged $PrP^{Scr106-126}$ (5μM) was dissolved in culture medium, centrifuged at 1000g for 10 minutes to eliminate large aggregates, and the supernatant was added to the cells. Every three days, the cells were trypsinized and sub-cultured with fresh peptide solution.

3.3. Immunofluorescence staining and confocal microscopy

For all immunostaining experiments, anti-PrP antibody 8H4 was used for detecting cellular PrP. This antibody is specific to residues 145-180 of PrP, and thus does not react with $PrP^{106-126}$. For detecting $PrP^{106-126}$ or $PrP^{Scr106-126}$, streptavidin-conjugated-Texas red was used due to the specific binding of streptavidin with biotin. For immunostaining cell surface proteins, permeabilization of the membrane with Triton X-100 was omitted. NT-2 cells cultured in normal medium, or 5μM of $PrP^{106-126}$ or $PrP^{Scr106-126}$ were fixed and stained with 8H4 (1:25)-anti-mouse-FITC (1:25) (Southern Biotechnology Associates), followed by streptavidin-conjugated-Texas red (1:40) (Pierce). For intracellular staining, fixed cells were permeabilized with 0.1% Triton X-100 prior to immunostaining as above. Stained cells were incubated with Hoechst 33342 (1μg/ml) (Molecular Probes) for five minutes to detect apoptotic nuclei, and mounted in gel-mount (Biomeda Corp., Fostar City, CA). All samples were observed with a Laser Scanning Confocal Microscope (BioRad MRC 600). A single 5μm optical section, and a composite of several sections were evaluated in each case.

3.4. Electron microscopy

For immunoelectron microscopy, control and $PrP^{106-126}$-treated cells were fixed in 4% paraformaldehyde and 0.01% glutaraldehyde, and immunostained with 8H4 (1:20 dilution), followed by peroxidase-conjugated anti-mouse (1:50) and mouse PAP (1:250). After washing with PBS, the cells were exposed to 3,3'-diaminobenzidine (DAB) containing 0.1M imidazole to obtain an electron-dense reaction product, and fixed again with 2.5% glutaraldehyde. Subsequently, the cells were post-fixed in 1% osmium tetroxide, dehydrated, embedded in Epon 812, and processed for electron microscopy. Post-staining with uranyl acetate and lead citrate was omitted to enhance the contrast for PrP-specific DAB stain. For intracellular immunostaining, fixed cells were permeabilized with 0.1% Triton X-100 before processing as above. For ultrastructural analysis, cells were fixed directly in the culture dish with a freshly prepared solution of 2.5% glutaraldehyde and post-fixed with 1% osmium tetroxide. Samples were rinsed in distilled water, block-stained in 0.5% uranyl acetate, dehydrated, and embedded in Epon as above. Thin sections were stained with uranyl acetate and lead citrate before examination with a Zeiss electron microscope (Zeiss CEM 902; Carl Zeiss Inc., Thornwood, NY).

3.5. SDS-PAGE and Western Blotting

Control and $PrP^{106-126}$-treated NT-2 cells were processed for Western blotting as described (22). In short, cells were lysed, and the precipitated proteins were electrophoretically transferred to Immobilon-P (Millipore) for 2.5 hours at 70 volts at 4°C. Membranes containing transferred proteins were probed with either anti-PrP antibody 8H4 (1:1000) followed by anti-mouse-HRP (1:4000), or streptavidin-conjugated HRP (1:40,000).

Reactive bands were visualized on an autoradiographic film by ECL (Amersham).

3.6. Metabolic labeling and immunoprecipitation

Control and peptide-treated cells were radiolabeled with 50μCi/ml of Trans^{35}S-label overnight in DMEM containing 5% dialyzed serum. The cells were washed with PBS, and incubated with 1μl/ml of PI-PLC (Oxford Glycosystems) in Opti-MEM for 1 hour at 37^{o}C. PI-PLC-released proteins in the medium, and cell lysates were subjected to immunoprecipitation with the anti-PrP antibody 3F4 or 8H4 as described (22, 23). 3F4 binds to residues 109 and 112 of PrP that are included in the truncated ^{Ctm}PrP and the conventional PK-resistant 20kDa fragment of PrP, and helps to distinguish these fragments from the 18kDa C-terminal fragment that is a product of normal PrP processing in the endosomes (24). Anti-PrP antibodies 8H4 and 2301 bind to both 18 and 20kDa fragments.

3.7. Assay of detergent insolubility and proteinase-K resistance

Aggregation, insolubility in non-ionic detergents, and partial resistance to proteinase K (PK) digestion are the hallmarks of PrP^{Sc}. To assay detergent insolubility, control, or peptide treated cells were lysed in a buffer containing non-ionic detergents NP-40 (1%) and DOC (0.5%). Large aggregates and nuclei were pelleted by low speed centrifugation at 500g, and the low-speed supernatant was further ultra-centrifuged at 100,000g in a Beckman SW50 rotor for 1 hour at 4^{o}C. The low and high-speed pellet and supernatant samples were analyzed by Western blotting. Duplicate sets of samples were electroblotted, and probed with 8H4 or streptavidin-HRP as above. Only the low speed fraction is shown here.

For evaluation of PK-resistance, lysates of control and PrP$^{106\text{-}126}$ treated cells were exposed to 3μg/ml of PK for 0, 2, or 4 minutes at 37^{o}C. The reaction was stopped with 1mM PMSF, and proteins were electroblotted and probed with 3F4 as described (20).

3.8. Cell homogenization and PK-treatment

Control and peptide-treated cells were washed and homogenized on ice in a buffer containing 10mM HEPES (pH7.9), 1.5mM $MgCl_2$, 10mM KCl, and 0.5mM DTT by 10 strokes of a Kontes all glass Dounce homogenizer. The homogenate was checked microscopically for cell breakage and centrifuged to pellet nuclei. The resulting supernatant was centrifuged at 20,000g to pellet membrane vesicles. These were re-suspended in 0.5ml of transport buffer (25mM HEPES pH7.4, 115mM KoAc, 2.5mM $MgCl_2$, 10mM KCl, 2.5mM $CaCl_2$, and 1mM DTT), and treated with 20μg/ml of proteinase-K on ice for 30 minutes. After adding 5mM of PMSF to stop the reaction, membrane vesicles were pelleted, solubilized in lysis buffer, and immunoblotted with 3F4.

3.9. Staining with Thioflavin S

Untreated control, and cells treated with PrP$^{106\text{-}126}$ for 1 year were fixed and permeabilized as above, and immunostained with 8H4 (1:25 dilution)-anti-mouse-RITC (1:40 dilution). Subsequently, the cells were incubated with a 1% aqueous solution of thioflavin-S for 20 minutes, washed three times with PBS, followed by one quick wash with 70% ethanol. Cells stained only with thioflavin S were pre-stained with the basic dye hematoxylin to reduce the background binding to nucleic acids, and processed as above.

4. RESULTS

4.1. PrP$^{106\text{-}126}$ induces the aggregation and internalization of cell surface PrP^{C}

To study the effect of long-term exposure of cells to PrP$^{106\text{-}126}$, NT-2 cells expressing high levels of PrP^{C} were cultured for 1-12 months in complete medium containing 5μM of PrP$^{106\text{-}126}$ biotinylated at the N-terminus. The cells were sub-cultured every three-five days with a fresh solution of the peptide. Cell viability and cell division was monitored to ensure that the peptide is not toxic to the cells under these conditions.

Interaction of PrP$^{106\text{-}126}$ with NT-2 cells was studied by immunofluorescence staining. Monoclonal antibody 8H4 was used to detect cellular PrP^{C}, and Texas-red-conjugated streptavidin to visualize biotin-tagged PrP$^{106\text{-}126}$. Since the epitope for 8H4 is between residues 145-180 of PrP, it does not bind PrP$^{106\text{-}126}$, and provides a convenient method to differentiate between PrP^{C} and PrP$^{106\text{-}126}$. After 1 month of exposure to PrP$^{106\text{-}126}$, cells were fixed with paraformaldehyde, and immunostained for PrP^{C} (green) or PrP$^{106\text{-}126}$ (red). For visualizing surface proteins, permeabilization with detergent was omitted. Small to large aggregates of PrP$^{106\text{-}126}$ are evident on the cell surface (red), most of which co-localize with PrP^{C} (yellow) (Figure 1, panel 2). Control cells cultured with scrambled PrP$^{106\text{-}126}$ show no staining for the peptide, but a uniform surface staining for PrP^{C} (Figure 1, panel 1). Permeabilization of cells before immunostaining shows large intracellular aggregates of PrP^{C} (green), PrP$^{106\text{-}126}$ (red), and mixed aggregates of PrP^{C} and PrP$^{106\text{-}126}$ (yellow) in PrP$^{106\text{-}126}$-treated cells (Figure 1, panel 4), whereas control cells show only a small amount of PrP immunoreactivity in the Golgi area (Figure 1, panel 3).

These results were confirmed by immunoelectron microscopy. Cells were fixed, permeabilized, and immunostained with 8H4. The bound antibody was reacted with appropriate secondary antibody and *di*aminobenzidine (DAB) to obtain an electron-dense deposit. Subsequent staining with uranyl acetate and lead citrate was omitted to obtain a better contrast with DAB staining. Cells cultured with scrambled peptide show a uniform distribution of PrP^{C} on the cell surface (Figure 1, panel 5), whereas PrP$^{106\text{-}126}$ treated cells show large intracellular aggregates of PrP^{C} enclosed by a membrane (Figure 1, panel 6).

These results show that exogenously added PrP$^{106\text{-}126}$ induces the aggregation and internalization of cell surface PrP^{C} in large membrane-bound vesicles. These aggregates degrade slowly, and persist even after one week of chase in normal medium (data not shown).

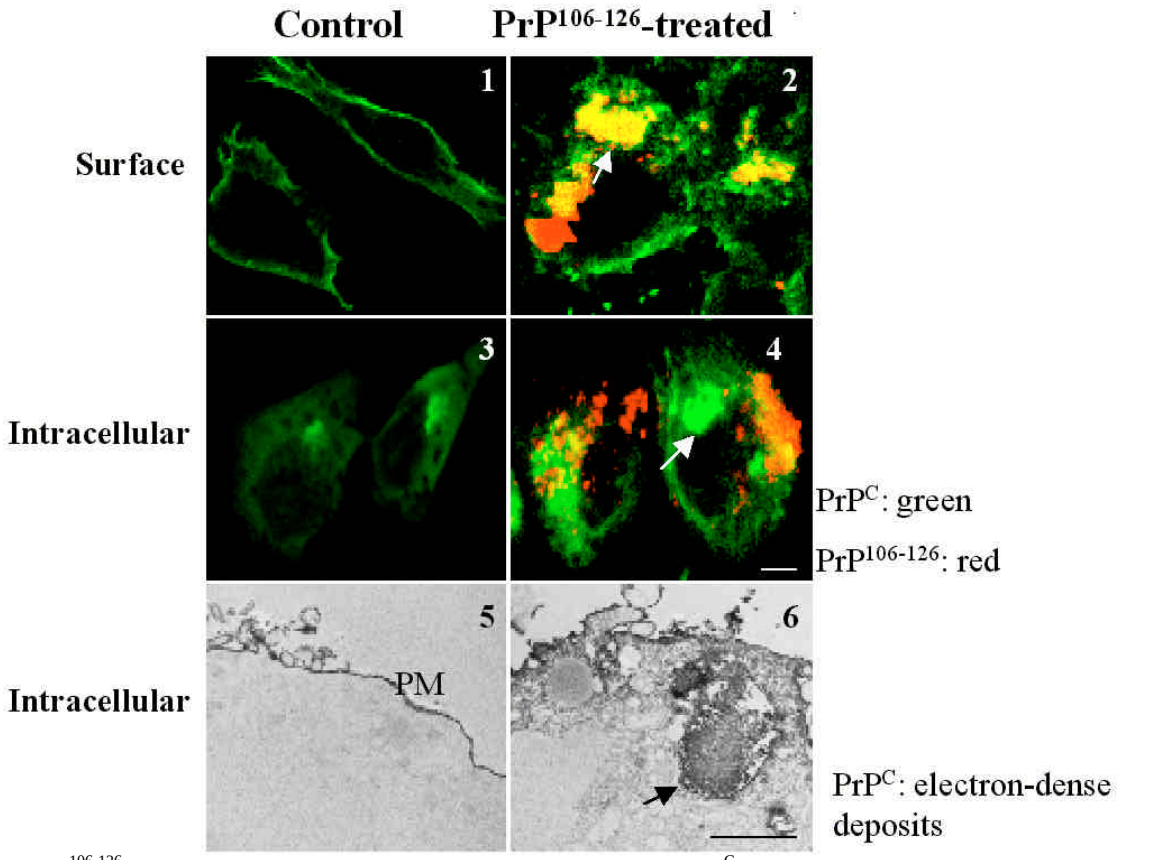

Figure 1. $PrP^{106-126}$ induces the aggregation and internalization of cell surface PrP^{C}. Surface immunofluorescence analysis of NT-2 cells treated with biotin-$PrP^{106-126}$ for 1 month with 8H4-FITC to identify PrP^{C} (green), followed by Texas-red-Streptavidin to detect biotin-$PrP^{106-126}$ (red) shows co-localization of PrP^{C} and $PrP^{106-126}$ aggregates on the plasma membrane (panel 2). Similar immunostaining of control cells treated with biotin-$PrP^{Scr106-126}$ for a similar period of time with 8H4 shows normal pattern of PrP immunoreactivity on the cell surface and in the Golgi area (panel 2). Similar analysis following permeabilization with Triton X-100 shows large intracellular aggregates of PrP^{C} (green), $PrP^{106-126}$ (red), or mixed aggregates (yellow) in treated cells (panel 4), whereas control cells show a small amount of immunoreaction in the Golgi area (panel 3). Bar, panels 1-4: 10µm. Immunoelectron microscopy of the above cells following permeabilization with triton X-100 shows a uniform, punctate staining of PrP^{C} on the surface of control cells treated with biotin-$PrP^{Scr106-126}$ (panel 5). In contrast, cells treated with biotin-$PrP^{106-126}$ show large intracellular aggregates of PrP^{C} that are enclosed by a membrane (panel 6). PM: plasma membrane; N: nucleus. Bar: 1µm. There are no obvious signs of cellular toxicity like swollen mitochondria or condensation of nuclear chromatin in treated cells (panel 6).

4.2. Aggregates of PrP^{C} are insoluble in non-ionic detergents

Insolubility in non-ionic detergents is one of the earliest changes observed during the transition of PrP^{C} to PrP^{Sc}. Conventionally, this is determined by preparing cell lysates in a buffer containing NP40 (1%) and DOC (0.5%), and subjecting lysates clarified at low speed to ultracentrifugation at 100,000g. Aggregated PrP is detected in the pellet fraction of ultracentrifuged samples. To check if the PrP^{C} deposits observed in Figure 1 are aggregated, control and treated cells cultured in the presence of $PrP^{106-126}$ for 1-12 months were subjected to the above treatment, and the pellet and supernatant fractions from low and high-speed centrifugation were immunoblotted with streptavidin or 8H4 to detect $PrP^{106-126}$ or PrP^{C} respectively. Only the low speed lysate obtained after centrifugation at 500g is shown in Figure 2, since almost all of the aggregated PrP from peptide-treated cells partitions in this fraction. PrP^{C} is soluble in non-ionic detergents, and is therefore also detected in the low speed fraction (Figure 2, lanes 3 and 4). In contrast, most of the $PrP^{106-126}$ and aggregated PrP^{C} from peptide treated cells is detected in the stacking gel of this fraction (Figure 2, lanes 2 and 4, top arrows). PrP-reactive protein aggregates in peptide-treated cells are too large to be resolved by the stacking or the separating gel, and cross-react with streptavidin, indicating that these are complex aggregates of PrP^{C} and $PrP^{106-126}$ (Figure 2, lanes 2 and 4, top arrows). A significant amount of monomeric, detergent-soluble $PrP^{106-126}$ is detected at ~3kDa in peptide-treated lysates, confirming that the $PrP^{106-126}$ added to the culture medium is not pre-assembled into large aggregates (Figure 2, lane 2, bottom arrow). Thus, most of the PrP^{C} aggregates in peptide-treated cells are large and insoluble in non-ionic detergents and SDS.

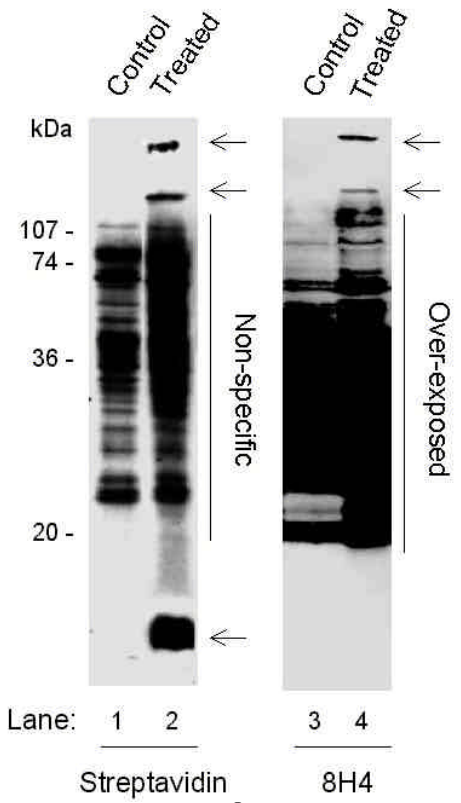

Figure 2. Aggregates of PrP^{C} are insoluble in non-ionic detergents. Lysates prepared from M17 cells treated with biotin-$PrP^{Scr106-126}$ (control) or biotin-$PrP^{106-126}$ (treated) for 4-12 months were centrifuged at low speed (500g), and immunoblotted with streptavidin (lanes 1 and 2), or 8H4 (lanes 3 and 4). Biotin-$PrP^{106-126}$-treated samples show protein aggregates in the stacking gel and at the top of separating gel that immunoreact with streptavidin (lane 2), and with 8H4 (lane 4). These aggregates are notably absent in control lysates (lanes 1 and 3). A 3kDa band of monomeric $PrP^{106-126}$ can be detected by streptavidin in treated cells (lane 2) which, as expected, immunoreacts only with streptavidin. (Reproduced from Ref. 25)

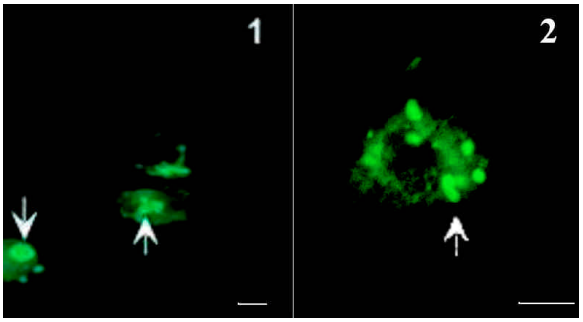

Figure 3. Intracellular $PrP^{106-126}$ and PrP^{C} aggregates bind Thioflavin-S. M17 cells treated with biotin-$PrP^{106-126}$ were fixed, permeabilized with Triton X-100, and stained with Thioflavin-S to detect amyloid. Green fluorescence of Thioflavin-S positive aggregates of different sizes is seen in vesicular structures, some more intense than others (panels 1 and 2). Bar: 25μm. (Reproduced from Ref. 25).

4.3. Internalized $PrP^{106-126}$ and PrP^{C} aggregates bind the amyloid-specific dye Thioflavin-S

To evaluate if intracellular aggregates of $PrP^{106-126}$ and PrP^{C} acquire the characteristics of amyloid, M17 and NT-2 cells treated with $PrP^{106-126}$ for 1 year were fixed with paraformaldehyde, permeabilized with detergent, and stained with the basic dye hematoxylin, followed by the amyloid binding dye thioflavin-S. Green fluorescence of thioflavin-stained aggregates can be seen in intracellular structures (Figure 3, panels 1 and 2), similar to the large endocytic vesicles observed in Figure 1 above. Co-immunostaining with 8H4 followed by RITC-conjugated secondary antibody shows that most of the thioflavin-positive aggregates co-immunostain for PrP^{C} (data not shown, 25). Thus, intracellular aggregates of PrP^{C} and $PrP^{106-126}$ acquire some of the characteristics of amyloid.

4.4. A C-terminal 20kDa fragment of ^{Ctm}PrP accumulates on the surface of peptide-treated cells

To investigate the metabolism of aggregated PrP^{C} in peptide treated cells, equal number of control, NT-2, and neuroblastoma cells treated with $PrP^{106-126}$ for 4-12 months were radiolabeled with ^{35}S-methionine overnight, and treated with PI-PLC to cleave cell surface GPI-linked proteins. Both the lysate and PI-PLC released samples were subjected to immunoprecipitation with anti-PrP antibody 3F4. Results obtained in neuroblastoma cells are shown in Figure 4 since these cells express considerably more PrP^{C} than NT-2 cells and the immunoprecipitation analysis is clearer in these cells. Analysis by SDS-PAGE fluorography shows significantly more PrP in the lysate sample of peptide-treated cells compared to controls, indicating that some of the intracellular accumulated PrP^{C} is soluble and immunoprecipitable before it aggregates and forms amyloid deposits (Figure 4, lanes 1 and 2). The amount of PrP^{C} released from the cell surface is similar in control and treated cells, except for a significant increase in the 20kDa fragment of PrP in peptide treated cells (Figure 4, lanes 3 and 4). Similar results on neuroblastoma cells treated with $PrP^{106-126}$ peptide were reported by us in a previous study (25).

Previous reports have documented that PrP^{C} exists in different topological forms at the endoplasmic reticulum (ER). Increased synthesis of one of the transmembrane forms, ^{Ctm}PrP, is believed to mediate the neurodegeneration observed in some inherited and infectious prion disorders (8, 9). As opposed to PrP^{C}, ^{Ctm}PrP is inserted in the ER membrane through its hydrophobic domain consisting of residues 113-135, with its N-terminus in the cytosol and C-terminus in the ER lumen. Thus, proteinase K (PK) treatment of microsomes spares ~19kDa C-terminal fragment, which is significantly increased in brain tissue obtained from diseased animals (8). To determine whether the 20kDa fragment observed in peptide treated cells is the proteolytically cleaved ^{Ctm}PrP, microsomes prepared from peptide-treated neuroblastoma cells were treated with 20μg/ml of PK on ice for 30 minutes. The reaction was stopped with PMSF, and the microsomes were solubilized in detergent and subjected to immunoblotting with 3F4. As expected, full-length GPI-linked forms of PrP^{C} are protected from the protease

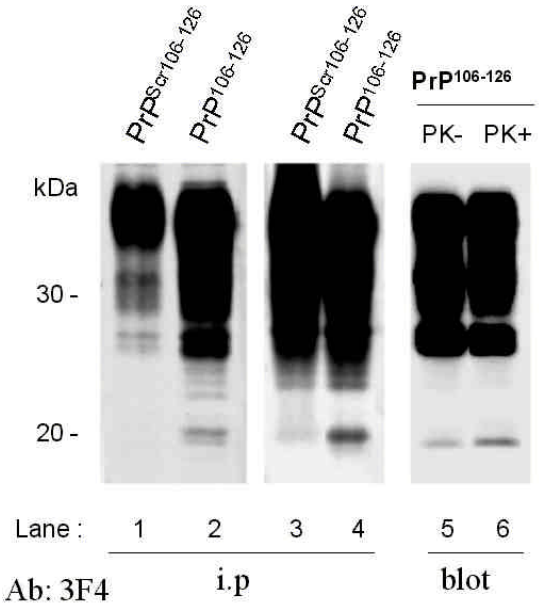

Figure 4. A C-terminal 20kDa fragment of ^{Ctm}PrP accumulates on the surface of PrP$^{106-126}$-treated cells. Neuroblastoma cells treated with biotin-PrP$^{Scr106-126}$ (control) or biotin-PrP$^{106-126}$ (treated) for 4-12 months were radiolabeled overnight with ^{35}S-methionine, and treated with PI-PLC to cleave surface-expressed PrP. Lysate and PI-PLC-released samples were immunoprecipitated with 3F4, and analyzed by SDS-PAGE-fluorography. The amount of PrP^{C} immunoprecipitated from treated cells is significantly more compared to control cells (lanes 1 vs 2). The 20kDa fragment of PrP is detected mainly in treated cells (lane 2), but is significantly more in PI-PLC released sample compared to cell-associated proteins (lanes 2 vs 4). Cells treated with biotin-PrP$^{106-126}$ for 4-12 months were homogenized, and resulting microsomes were treated with 20μg/ml of PK for 30 minutes on ice. After inactivating PK, microsomes were solubilized with detergent, and immunoblotted with 3F4. As expected, full-length PrP^{C} is protected from PK-digestion, but the amount of 20kDa fragment increases in amount after PK treatment (lanes 5 and 6). (Reproduced From Ref. 25)

(Figure 4, lanes 5 and 6). In contrast, there is a small but significant increase in the 20kDa fragment after PK treatment of peptide-treated cells (Figure 4, lanes 5 and 6), indicating that the 20kDa fragment is generated by limited proteolysis of ^{Ctm}PrP. Similar results were obtained with NT-2 cells.

The above results show that the synthesis of ^{Ctm}PrP is upregulated in peptide treated cells. Furthermore, ^{Ctm}PrP is spontaneously cleaved on the cytosolic face of the ER membrane to release the C-terminal 20kDa fragment, which is transported to the plasma membrane.

4.5. Isolation of PrP$^{106-126}$-resistant mutants

To dissect the biochemical pathways of neurotoxicity by PrP$^{106-126}$, mutant cells that are resistant to toxicity by this peptide were isolated. Neuroblastoma and NT-2 cells were chosen for these experiments. Neuroblastoma cells express high amounts of PrP and are easy to expand and maintain in culture, and NT-2 cells, a human teratocarcinoma cell line has the advantage that it can be differentiated into mature human neurons (NT-2N) by a series of treatments with retinoic acid, and mimics primary human neuronal cultures closely (42). After full differentiation, NT-2N cells still express detectable amounts of PrP, and ~95% of the cells stain positive for the neuronal marker NF68. Before proceeding with the selection of resistant cells, we confirmed that the differentiated NT-2N cells are as sensitive to PrP$^{106-126}$ treatment as undifferentiated NT-2 cells.

To isolate resistant cells, neuroblastoma and NT-2 cells were exposed to the mutagens MNNG or EMS, and the dose that killed ~50% of the cells were chosen for further selection. Cells exposed to the mutagens were cultured in regular medium for one week to obtain healthy cultures. Subsequently, mutagenized, and non-mutagenized control cells were exposed to the constant presence of 80μM of PrP$^{106-126}$ or PrP$^{Scm106-126}$ in complete medium for a period of 3-4 weeks. Cell-death was monitored by checking lactate-dehydrogenase (LDH) activity released into the medium. During the first week of treatment, LDH released into the medium continued to rise in control (NT-2), and NT-2 mutagenized with MNNG or EMS. Subsequently, LDH values continued to rise in NT-2 cells till all the cells died after 5-6 weeks. In mutagenized cells, the LDH values started to decrease after one week, and were virtually similar to untreated samples at the end of six weeks. The mutant cells that survived PrP$^{106-126}$ treatment were expanded in the constant presence of the peptide. PrP$^{106-126}$-resistant neuroblastoma cells were selected in a similar fashion, and checked by re-exposing to toxic doses of the peptide. As shown in Figure 5, although the cells are engorged with large aggregates of PrP$^{106-126}$, the cell viability is not compromised, as assessed by nuclear staining with the chromatin binding dye Hoechst (Figure 5, panels 2 and 3).

4.6. Preliminary characterization of PrP$^{106-126}$-resistant cells

To check for differences in the expression of any major cellular proteins in the resistant cells, control and resistant cells were labeled with ^{35}S-methionine/cysteine for 2 hours, lysed with detergent, and the radiolabeled proteins precipitated by cold methanol were analyzed by SDS-PAGE-fluorography. Only a minor quantitative difference in the protein band migrating at ~18kDa is detected between the control and PrP$^{106-126}$-resistant NT-2 cells mutagenized with EMS (NT-2ER) or MNNG (NT-2MR) (Figure 6, lanes 1-3). No detectable differences were noticed in resistant neuroblastoma cells (data not shown). An analysis of the difference in mRNA pattern between the control and mutant cells by differential display analysis is under way.

To assess for any differences in the uptake and intracellular distribution of PrP$^{106-126}$ by the resistant cells, PrP$^{106-126}$-resistant NT-2 cells were exposed to biotinylated PrP$^{106-126}$ for 10 days, and stained with texas-red-conjugated streptavidin. The resistant cells show a variety

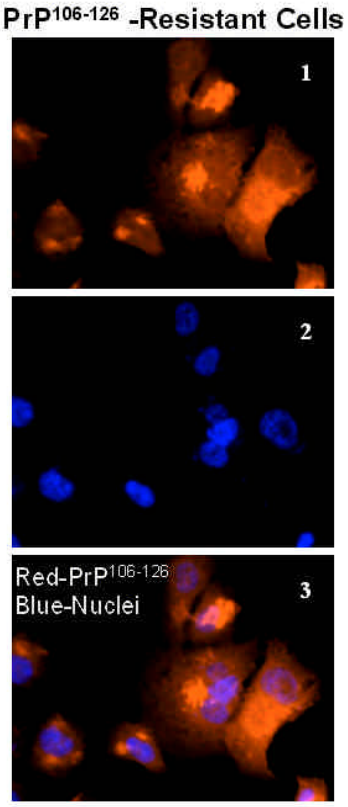

Figure 5. Resistant cells accumulate large aggregates of $PrP^{106-126}$ without toxicity. Co-staining of $PrP^{106-126}$-resistant NT-2 cells with the nuclear dye hoechst shows that despite the presence of large intracellular aggregates (panel 1), there is no nuclear fragmentation (panels 2 and 3).

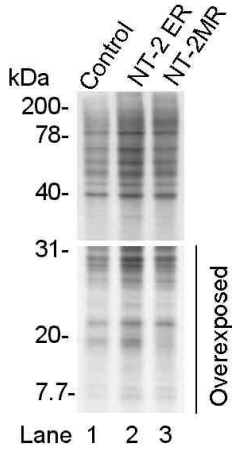

Figure 6. Protein expression pattern of control and resistant cells. Control and $PrP^{106-126}$-resistant NT-2 cells mutagenized with EMS (NT-2ER) or MNNG (NT-2MR) were incubated with ^{35}S-methionine/cysteine for 2 hours to metabolically label all cellular proteins. Radiolabeled proteins were precipitated with cold methanol, and analyzed by SDS-PAGE-fluorography. Lower half of the gel is over-exposed to visualize the protein bands better. As compared to control cells (lane 1), a protein band ~ 18kDa is absent in NT-2MR cells (lane 3).

of distribution patterns of PrP106-126. Some cells fail to internalize the peptide, which is seen at the cell surface (Figure 7, panels 1 and 2). Others have large intracellular aggregates of PrP106-126 without any apparent toxic effects on the cell (Figure 7, panels 3 and 4). Although several cells show large intracellular aggregates, no nuclear fragmentation was detected when stained with the chromatin-binding dye Hoechst (data not shown). These cells are presently being cloned in order to evaluate the specific biochemical changes that confer PrP106-126-resistance to these cells.

5. DISCUSSION

This study broadens our understanding of the possible mechanisms of PrP replication and PrP^{Sc}-induced neurotoxicity in significant ways. First, we show that a β-sheet-rich 'seed' of PrP can initiate the accumulation of full-length PrP^{C} into detergent-insoluble aggregates, confirming the nucleation hypothesis of PrP^{Sc} formation. Second, we demonstrate that intracellular aggregates of PrP increase the synthesis of ^{Ctm}PrP, implicating ^{Ctm}PrP as an important mediator of PrP^{Sc} pathogenicity. And finally, we describe the isolation of neuronal cells that are resistant to toxicity by PrP peptide 106-126, providing a unique opportunity to dissect the pathways of neurotoxicity by this peptide, and by extension, PrP^{Sc}.

By exposing cultured NT-2 and neuroblastoma cells to non-toxic concentrations of PrP106-126, we demonstrate a change in conformation of endogenous PrPC into a PrPSc-like form. While the cellular and biochemical processes that mediate neuronal toxicity by PrPSc are still unclear, substantial evidence indicates that propagation of PrPSc occurs through the conversion of host PrPC into its own conformation. Two hypotheses have been proposed to explain the mechanism of this conformational change: 1) template-assisted re-folding of endogenous PrPC to PrPSc, and 2) the nucleation or seeding hypothesis (26, 27). We show that a ? -sheet-rich internal fragment PrP106-126 seeds the aggregation of PrPC on the plasma membrane, and catalyzes its accumulation in an exponential manner. We believe that PrP106-126 incorporates within the lipid bilayer, where the charged phospholipid environment induces its aggregation. Subsequently, it acts as a seed for the deposition of additional PrPC molecules. Since ? -sheet rich peptides have an affinity for cholesterol (10, 28), aggregated PrP106-126 probably concentrates in cholesterol-rich lipid domains of the plasma membrane, which is also the sub cellular location for the conversion of PrPC to PrPSc (29-31), thus providing an ideal environment for the conversion to PrPSc.

After the initial conformational change, PrP^{C} and $PrP^{106-126}$ aggregates are transported to the endosomal/lysosomal compartment, where low pH and the negatively charged membrane microenvironment probably plays a major role in promoting their transformation to thioflavin-S-binding, ? -sheet rich, amyloidogenic structures. The accumulation of these virtually undegradable PrP^{C} and $PrP^{106-126}$ aggregates explains the extensive proliferation of lysosomes observed in our cell model (25), and the presence of abundant PrP immunoreactive lysosomes in the neurons of

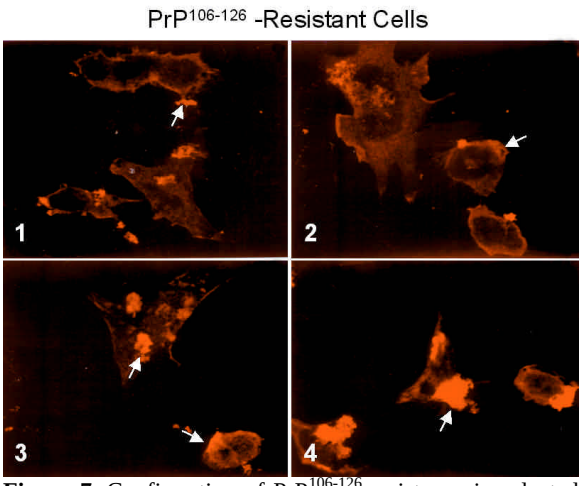

Figure 7. Confirmation of $PrP^{106-126}$-resistance in selected cells. $PrP^{106-126}$-resistant NT-2 cells were re-exposed to $PrP^{106-126}$ for 10 days, fixed, permeabilized, and stained with Texas-red conjugated streptavidin. Some cells show surface staining of the peptide (panels 1 and 2, arrows), whereas others contain large intracellular aggregates (panels 3 and 4).

scrapie-infected animals and New Variant Creutzfeldt Jakob Disease patients (29, 32). A similar change in conformation from an α-helical to a β-sheet structure has been reported for recombinant PrP^{91-231} and for certain other peptides when exposed to an acidic pH (1, 33).

The intracellular aggregates of PrP^{C} generated in our model display the essential biochemical characteristics of PrP^{Sc}, including detergent insolubility, and partial resistance to digestion by proteinase K (PK) (25). In fact, most of the aggregated PrP^{C} is insoluble even in SDS, and cannot be resolved by conventional SDS-PAGE. It is plausible that these aggregates travel along axons to neighboring cells by vesicular traffic, or alternately, are extruded into the extracellular milieu and are subsequently internalized by other cells. Microglia cultured in the presence of Aβ show similar results (34). Since most of the PrP^{Sc} in diseased brains is probably sequestered in plaques, the propagation of PrP^{Sc} may occur through fragments like $PrP^{106-126}$ that are relatively soluble, resistant to proteases, and have the potential to fold into β-sheet upon contact with the membrane micro-environment. The occurrence of such a phenomenon would explain the exponential spread of PrP^{Sc} infection in the brain.

This study shows that intracellular accumulation of PrP^{Sc} upregulates the synthesis of ^{Ctm}PrP, the proposed mediator of PrP^{Sc}-induced neurodegeneration. There is a significant increase in the surface expression of C-terminal 20kDa fragment of PrP in peptide-treated cells, similar to the fragment of ^{Ctm}PrP obtained above after PK treatment (8, 9). We believe that this fragment is a result of spontaneous truncation of ^{Ctm}PrP at the endoplasmic reticulum (ER) membrane. Consistent with our observations, an increase of ^{Ctm}PrP expression has been reported in the brains of mice infected with PrP^{Sc} by using an indirect method (9). The truncated ^{Ctm}PrP molecules thus generated are transported to the cell surface and inserted in the plasma membrane by the GPI anchor (25).

The mutant cells resistant to toxicity by the PrP fragment 106-126 reported in this study are a unique model to understand the biochemical pathways of neurotoxicity by this fragment, and PrP^{Sc}. Several lines of evidence indicate the validity of this model system. A number of studies have demonstrated that $PrP^{106-126}$ causes neuronal death by apoptosis when added to primary cultures of neurons (35-37). Although the biochemical events mediating neurotoxicity by this fragment are not clear, the region encompassing residues 112-126 is believed to be essential for the neurotoxic effect of this peptide (38). A similar phenomenon of neurotoxicity is observed when neuronal cells are exposed to PrP^{Sc} (39, 40). Moreover, this region of PrP seems to play a central role in the conversion of PrP^{C} to PrP^{Sc}. For example, a PrP peptide including residues 106-141 can block the conversion of PrP^{C} to PrP^{Sc} in an *in vitro* conversion reaction, probably by competitively binding to PrP^{C}, or by blocking the interaction of PrP^{C} and PrP^{Sc} (15, 41). Residues 113-120 seem to be especially critical for this inhibitory effect, and the inhibition of conversion is independent of the peptide's ability to form β-sheets. PrP peptides including residues 90-145 have been shown to induce aggregation, high β-sheet content, and PK-resistance in PrP^{C} *in vitro* (13), and PrP109-122 can induce the transition from α-helix to β-sheets in other PrP peptides (14). Additional evidence for the critical role of this region of PrP in the conversion of PrP^{C} to PrP^{Sc} is derived from the fact that mutant mouse PrP lacking residues 114-121 is not converted to the scrapie form after expression in scrapie infected mouse neuroblastoma cells (16). Thus, $PrP^{106-126}$ closely parallels cellular events that follow the exposure of PrP^{Sc} to neuronal cells. By isolating cell clones resistant to toxicity by this peptide, we will be able to identify specific biochemical pathways mediating the neurotoxicity of PrP^{Sc}. We chose the human neuroblastoma M17 transfected with PrP, and NTera-2 (NT-2), a human teratocarcinoma cell line that can be differentiated into mature human neurons for isolating $PrP^{106-126}$-resistant cells (42). M17 cells are easy to maintain in culture and large quantities can be obtained in a short time, whereas NT-2 cells offer the opportunity of analyzing a pure population of mature human neurons. Since primary brain cultures are usually a mixture of nerve cells and glial populations, this cell system offers several advantages over existing methods used to analyze the toxicity of PrP106-126. Undifferentiated NT-2 cells can be grown in culture with relative ease, and upon differentiation with retinoic acid, are a constant source of ~95-100% pure culture of mature human neurons (42). Therefore, mutagenesis and several of the preliminary experiments can be performed on NT-2 cells, and then confirmed in differentiated cells (NT-2N). Biochemical and genetic studies are also more feasible in NT-2 or NT-2N cells than primary cultures of central nervous system neurons, which are difficult to obtain in large quantities, and are heavily contaminated with other cells. Moreover, NT-2N cells can be engrafted in the brains of nude mice, where they can survive for several months

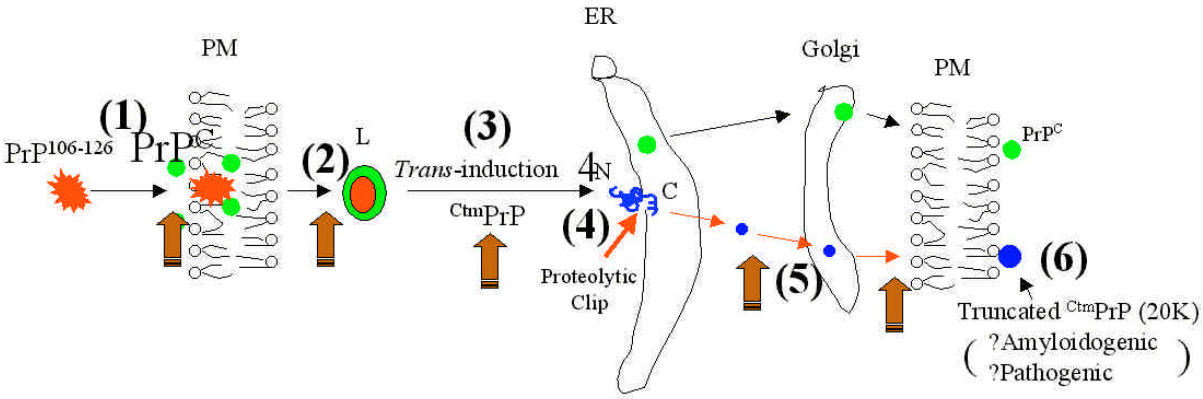

Figure 8. Proposed model of PrP^{C} propagation and neurotoxicity. (1), micro-aggregates of $PrP^{106-126}$ bind to the plasma membrane and initiate the aggregation of PrP^{C}. (2), the aggregated proteins are endocytosed in large vesicular structures, and transported to lysosomes. (3), the intracellular PrP aggregates induce the synthesis of ^{Ctm}PrP through *trans*-activating factors. (4), through as yet unknown mechanism, the N-terminal region of ^{Ctm}PrP is cleaved by cytosolic enzymes. (5), the C-terminal 20kDa fragment of ^{Ctm}PrP is transported to the cell surface through the secretory path. (6), the truncated ^{Ctm}PrP is inserted in the outer leaflet of the plasma membrane through the GPI anchor. Brown arrows indicate possible biochemical pathways that may be interrupted in $PrP^{106-126}$-resistant cells. PM, plasma membrane; ER, endoplasmic reticulum; L, lysosomes; ^{Ctm}PrP, transmembrane PrP.

(43). This procedure offers a unique opportunity to engraft $PrP^{106-126}$-resistant mutant cells in scrapie-infected nude mice carrying the human PrP transgene to evaluate if these cells will resist infection and toxicity *in vivo*.

Our results show that $PrP^{106-126}$ is internalized by M17 and NT-2 cells in a time and temperature-dependant fashion. On the cell surface, it does not appear to bind PrP, confirming earlier studies that the uptake of this peptide is not affected in PrP-deficient cells (44). However, contrary to a previous report (21), our results show that $PrP^{106-126}$ accumulates in the lysosomes, where it is relatively stable and forms large aggregates. After a prolonged exposure of the cells to $PrP^{106-126}$, it can also be detected in axon-like processes of both cells lines. Whether this is due to endocytosis of the peptide by axons or represents transport of the peptide from one cell to the next is not clear from our data. Transport of PrP^{Sc} through axons in scrapie-infected brains has been reported in earlier studies (45).

The $PrP^{106-126}$-resistant cell clones isolated in this study will help to clarify several outstanding questions, such as the role of oxidative damage, probably induced by activated microglia (37), the interaction of α- and β-tubulin with $PrP^{106-126}$ (44), and the importance of plasma membrane microviscosity and intracellular calcium levels in the toxicity mediated by this peptide (46, 47). Some of the $PrP^{106-126}$-resistant cells do not internalize the peptide, and may lack the receptor involved in the internalization of this peptide, whereas others contain large intracellular aggregates of this peptide with apparently no toxic effect on the cells. These cells probably differ from $PrP^{106-126}$-sensitive control cells in the biochemical pathway(s) mediating neurotoxicity by this peptide. We are presently carrying out complementation studies with different clones to identify the biochemical abnormalities that confer the resistant phenotype to these cells. We believe that an analysis of these clones will help to characterize the cellular and biochemical pathways that lead to cell death by $PrP^{106-126}$, and will provide insight into the mechanism of neurotoxicity by PrP^{Sc}.

6. ACKNOWLEDGMENTS

We thank Dr. P. Gambetti for his support, Dr. M.S. Sy and Ruliang Li for providing the anti-PrP 8H4 antibody, Dr. J. Anderson for the use of confocal microscope, Yi Jing, Yogesh Sharma, and Anil Kumar for technical help, and Hisashi Fujioka and Kiet Luc for assistance with electron microscopy. This work was supported by National Institutes of Health grants NS35962 and NS39089 (to N.S).

7. REFERENCES

1. Prusiner, S. B : Molecular biology and pathogenesis of prion disease. *Trends Biochem. Sci* 21, 482-487 (1996)
2. Prusiner, S. B: Prions. *Proc. Natl. Acad. Sci. USA* 95, 13363-13383 (1998)
3. Cohen, F. E. & S. B. Prusiner: Pathologic conformations of prion proteins. *Annu. Rev. Biochem* 67, 793-819 (1998)
4. Caughey, B: Transmissible spongiform encephalopathies, amyloidoses and yeast prions: Common threads? *Nat. Med* 6, 751-754 (2000)
5. Brown, P. Gibbs, C. J. Rodgers-Johnson, P. Asher, D. M. Sulima, M.P. Bacote, A. Goldfarb, L.G. & D.C. Gajdusek: Human spongiform encephalopathy: the National Institutes of Health series of 300 cases of experimentally transmitted disease. *Annal. Neurol* 35, 513-529 (1994)
6. Tateishi, J & T. Kitamoto: Inherited prion diseases and transmission to rodents. *Brain Pathol* 5, 53-59 (1995)
7. Tateishi, J. Kitamoto, T. Hoque, M.Z. & H. Furukawa : Experimental transmission of Creutzfeldt-Jakob disease

and related disorders to rodents. *Neurology* 40, 1578-1581(1996)
8. Hegde, R. S. Mastrianni, J. A. Scott, M. R. DeFea, K. A. Tremblay, P. Torchia, M. DeArmond, S. J. Prusiner, S. B. & V.R. Lingappa: A transmembrane form of the prion protein in neurodegenerative disease. *Science* 279, 827-834(1998)
9. Hegde, R. S. Trembly, P. Groth, D. DeArmond, S. J. Prusiner, S. B. & V.R. Lingappa: Transmissible and genetic prion disease share a common pathway of neurodegeneration. *Nature* (London) 402, 822-826 (1999)
10. Rymer, D. L. & T.A. Good: The role of prion peptide structure and aggregation in toxicity and membrane binding. *J. Neurochem* 75, 536-2545 (2000)
11. Ettaiche, M. Pichot, R. Vincent, J.-P. & J. Chabry: In vivo cytotoxicity of the prion protein fragment 106-126. *J. Biol. Chem* 275,36487-36490 (2000)
12. Brown, D.R : PrP^{Sc}-like prion protein peptide inhibits the function of cellular prion protein. *Biochem. J* 352, 511-518 (2000)
13. Kaneko, K. Peretz, D. Pan, K.-M. Blochberger, T. Wille, H. Gabizon, R. Griffith, O. H. Cohen, F. . Baldwin, M. A & S. B. Prusiner: Prion protein (PrP) synthetic peptides induce cellular PrP to acquire properties of the scrapie isoform. *Proc. Natl. Acad. Sci.* USA, 32,11160-11164 (1995)
14. Nguyen, J. Baldwin, M. A. Cohen, F. E. & S. B. Prusiner: Prion protein peptides induce α–helix to β–sheet conformation transitions. *Biochemistry* 34, 4186-4192 (1995)
15. Chabry, J. Caughey, B. & B. Chesebro: Specific inhibition of In Vitro formation of protease-resistant prion protein by synthetic peptides. *J. Biol. Chem* 273, 13203-13207(1998)
16. Holscher, C. Delius, H. & A. Burkle: Over-expression of non-convertible PrP^{c} β114-121 in scrapie-infected mouse neuroblastoma cells leads to transdominant inhibition of wild-type PrPSc accumulation. *J. Virol* 72, 1153-1159 (1998)
17. Martins, V. R. Graner, E. Gracia-Abreu, J. Souza, S. J. D. Mercadante, A. F. Veiga, S. S. Zanata, S.M. Neto,V. M & R. R. Brentani: Complementary hydropathy identifies a cellular prion protein receptor. *Nat. Med* 3 , 1376-1382 (1997)
18. Rieger, R. Edenhofer, F. Lasmezas, C. I. & S. Weiss: The human 37kDa laminin receptor precursor interacts with the prion protein in eukaryotic cells. *Nat. Med* 3, 1383-1388 (1997)
19. Zanusso, G. Liu, D. Ferrari, S. Hegyi, I. Yin, X. Aguzzi, A. Hornemann, S. Liemann, S. Glockshuber, R. Manson, J.C. Brown, P. Petersen, R.B. Gambetti, P. & M. S. Sy: Prion protein expression in different species: analysis with a panel of new mAbs. *Proc. Natl. Acad. Sci* USA 95, 8812-8816 (1998)
20. Singh, N. Zanusso, G. Chen, S. G. Fujioka, H. Richardson, S. Gambetti, P. & R. B. Petersen: Prion protein aggregation reverted by low temperature in transfected cells carrying a prion protein gene mutation. *J. Biol. Chem* 272, 28461-28470 (1997)
21. McHattie, S. J. Brown, D. R. & M. M. Bird: Cellular uptake of the prion protein fragment PrP106-126 in vitro. *J. Neurocytol* 28, 149-159 (1999)
22. Zanusso, G. Petersen, R. B. Jin, T. Jing, Y. Kanhoush, R. Ferrari, S. Gambetti, P. & N. Singh: Proteasomal degradation and N-terminal protease resistance of the codon 145 mutant prion protein. *J. Biol. Chem* 274 , 23396-23404 (1999)
23. Jin, T. Gu, Y. Zanusso, G. Sy, M. S. Kumar, A. Cohen, M. Gambetti, P. & N. Singh: The chaperone protein BiP binds to a mutant prion protein and mediates its degradation by the proteasome. *J. Biol. Chem* 275, 38699-38704 (2000)
24. Chen, S.G. Teplow, D.B. Parchi, P. Teller, J.K. Gambetti, P. & L. Autilio-Gambetti: Truncated forms of the human prion protein in normal brain and in prion diseases. *J. Biol. Chem* 270, 19173-19180 (1995)
25. Gu, Y. Fujioka, H. Mishra, R.S. Li, R. and N. Singh: Prion peptide 106-126 modulates the aggregation of cellular prion protein and induces the synthesis of potentially neurotoxic transmembrane PrP. *J. Biol. Chem* 277 2275-2286 (2002)
26. Jarret, J. T. & P. T. Lansbury: Seeding "one-dimensional crystallization" of amyloid: a pathogenic mechanism in Alzheimer's disease and scrapie? *Cell* 73, 1055-1058 (1993)
27. Horwich, A. L. & J. S. Weissmann: Deadly conformations-protein misfolding in prion disease *Cell* 89, 499-510 (1997)
28. Mizuno, T. Nakata, M. Naiki, H. Michikawa, M. Wang, R. Haas, C. & K. Yanagisawa: Cholesterol-dependent generation of a seeding amyloid β–protein in cell culture. *J. Biol. Chem* 274, 15110-15114 (1999)
29. Laszlo, L. Lowe, J. Self, T. Kenward, N. Landon, M. McBride, T. Farquhar, C. McConnell, I. Brown, J. Hope, J. & R. J. Meyer: Lysosomes as key organelles in the pathogenesis of prion encephalopathies. *J. Pathol* 166, 333-341(1992)
30. Taraboulos, A. Scott, M. Semenov, A. Avraham, D. Lazlo, L. & S. B. Prusiner: Cholesterol depletion and modification of COOH-terminal targeting sequences of the prion protein inhibit formation of the scrapie isoform. *J. Cell Biol* 129,121-132 (1995)
31. Naslavsky, N. Stein, R. Yanai, A. Friedlander, G. & A. Taraboulos: Characterization of detergent-insoluble complexes containing the cellular prion protein and its scrapie isoform. *J. Biol. Chem* 272, 6324-6331(1997)
32. Grigoriev, V. Haye, F. E. Streichenberger, N. Kopp, N. Langeveld, J. Brown, P. & J.-G. Fournier: Submicroscopic immunodetection of PrP in the brain of a patient with a new–variant of Creutzfeldt-Jakob disease. *Neurosci. Lett* 264, 57-60 (1999)
33. Hornemann, S. & R. Glockshuber: A scrapie-like unfolding intermediate of the prion protein domain PrP (121-131) induced by acidic pH. *Proc. Natl. Acad. Sci.* USA 95, 6010-6014 (1998)
34. Chung, H. Brazil, M. I. Soe, T. T. & F. R. Maxfield: Uptake, degradation, and release of fibrillar and soluble forms of Alzheimer's amyloid β-peptide by microglial cells. *J. Biol. Chem* 274,32301-32308 (1999)
35. Forloni, G. Angeretti, N. Chiesa, R. Monzani, E. Salmona, M. Bugiani, O. & F. Tagliavini: Neurotoxicity of a prion protein fragment. *Nature* (London) 362 , 543-545 (1993)
36. Forloni, G. Bugiani, O. Tagliavini, F. & M. Salmona: Apoptosis-mediated neurotoxicity induced by β-amyloid and

PrP fragments. *Mol. Chem. Neuropathol* 28, 163-171 (1996)
37. Brown, D. R. Schmidt, B. & H. A. Kretzschmar: Role of microglia and host prion protein in neurotoxicity of a prion protein fragment. *Nature* (London) 380, 345-347 (1996)
38. Brown, D. R.: Prion protein peptides: Optimal toxicity and peptide blockade of toxicity. *Mol. Cell Neurosci* 15, 66-78 (2000)
39. Muller, W. E. G. Ushijima, H. Schroder, H. C. Forrest, J. M. S. Schatton, W. F. H Rytik, P. G. & M. Heffner-Lauc: Cytoprotective effect of NMDA receptor antagonists on prion protein (PrP) Induced toxicity in rat cortical cell cultures. *Eur. J. Pharmacol* 246, 261-267(1993)
40. Giese, A. Brown, D. R. Groschup, M. H. Feldmann, C. Haist, I. & H. A. Kretzschmar: Role of microglia in neuronal cell death in prion disease. *Brain Pathol* 8, 449-457 (1998)
41. Kocisko, D. A. Come, J.H. Priola, S. A. Chesebro, B. Raymond, G. L. Lansbury, P. T. & B. Caughey: Cell free formation of protease resistant prion protein. *Nature* (London) 370 , 471-474 (1994)
42. Pleasure, S. J. Page, C. & V. M. Y. Lee: Pure postmitotic, polarized human neurons derived from Ntera 2 cells provide a system for expressing exogenous proteins in terminally differentiated neurons. *J. Neurosci* 12 , 1802-1815(1992)
43. Cotman, C.W. & J. H. Su: Mechanism of neuronal death in Alzheimer's disease. *Brain Pathol* 6 , 493-506 (1996)
44. Brown, D.R. Schmidt, B. & H. A. Kretzschmar: Prion protein fragment interacts with PrP-deficient cells. *J. Neurosci*. *Res* 52 , 260-267 (1998)
45. Jendroska, K. Heinzel, F. P. Torchia, M. Stowring, L. Kretzschmar, H. A. Kon, A. Stern, A. Prusiner, S. B. & S. J. DeArmond: Proteinase-resistant prion protein accumulation in Syrian hamster brain correlates with regional pathology and scrapie infectivity. *Neurology* 41, 1482-1490 (1991)
46. Salmona, M. Forloni, G. Diomede, L. Algeri, M. DeGioia, L. Angeretti, N. Giaccone, G. Tagliavini, F. & O. Bugiani: A neurotoxic and gliotrophic fragment of the prion protein increases plasma membrane microviscosity. *Neurobiol. Dis*. 4 , 47-57(1997)
47. Lin, M. C. Mirzabekov, T. & B. L. Kagan: Channel formation by a neurotoxic prion protein fragment. *J. Biol. Chem*. 272, 44-47 (1997)

Abbreviations: $PrP^{106-126}$: PrP peptide including residues 106-126 biotin-tagged at the N-terminus; $PrP^{Scr106-126}$: PrP peptide with a scrambled 106-126 sequence biotin-tagged at the N-terminus; PrP^{C}: normal cell associated PrP; PrP^{Sc}: conformationally transformed scrapie form of PrP; PK: proteinase K; PNGase-F: N-glycosidase-F; PI-PLC: phosphatidylinositol-specific phospholipase C

Key Words: Cell Biology, Prion Replication, Neurotoxicity

Send correspondence to: Dr Neena Singh, The Institute of Pathology, Case Western Reserve University, 2085, Adelbert Road, Cleveland, Ohio 44106. Tel: 216-368-2617, Fax: 216-368-2546, E-mail: nxs2@po.cwru.edu